Spectroscopic evidence of the existence of substantial Ca 3*d* derived states at the Fermi level in the Ca-intercalated graphite superconductor CaC_6

H. Okazaki,[1] R. Yoshida,[1] K. Iwai,[1] K. Noami,[1] T. Muro,[2] T. Nakamura,[2] T. Wakita,[3,4] Y. Muraoka,[1,3,4] M. Hirai,[1,3] F. Tomioka,[5] Y. Takano,[5] A. Takenaka,[6] M. Toyoda,[6] T. Oguchi,[7] and T. Yokoya[1,3,4]

[1]*The Graduate School of Natural Science and Technology, Okayama University, 3-1-1 Tsushima-naka, Okayama 700-8530, Japan*

[2]*Japan Synchrotron Radiation Research Institute (JASRI) and SPring-8, 1-1-1 Kouto, Sayo, Hyogo 679-5198, Japan*

[3]*Research Laboratory for Surface Science (RLSS), Okayama University, 3-1-1 Tsushima-naka, Okayama 700-8530, Japan*

[4]*CREST, Japan Science and Technology Corporation (JST), 3-1-1 Tsushima-naka, Okayama 700-8530, Japan*

[5]*National Institute for Materials Science (NIMS), 1-2-1 Sengen, Tsukuba, Ibaraki 305-0047, Japan*

[6]*Faculty of Engineering, Oita University, 700 Dannoharu, Oita 870-1192, Japan*

[7]*Department of Quantum Matter, Graduate School of Advanced Sciences of Matter (ADSM), Hiroshima University, 1-3-1 Kagamiyama, Higashi-Hiroshima, Hiroshima 739-8530, Japan*

(Received 30 October 2008; revised manuscript received 1 May 2009; published 16 July 2009)

We have performed soft x-ray photoemission studies of Ca-intercalated graphite superconductor CaC_6 (T_c=11.2 K). The valence-band spectrum shows six main structures, with a peak at the Fermi level (E_F), which correspond to those of calculated DOS. The intensity of the E_F peak is resonantly enhanced at the Ca 2*p*-3*d* threshold, providing spectroscopic evidence for the existence of Ca 3*d* electrons at E_F, which is confirmed experimentally for the first time. The Ca 2*p* core-level spectrum has a very large asymmetric line shape, which is further possible suggestion of the existence of Ca 3*d* derived conduction electrons at Ca sites. These results strongly support the picture where Ca 3*d* derived interlayer band plays a crucial role for the superconductivity of this material with relatively high T_c.

DOI: 10.1103/PhysRevB.80.035420 PACS number(s): 79.60.−i, 74.70.−b, 74.25.Jb

I. INTRODUCTION

Graphite intercalation compounds (GICs) are made by the insertion of atomic or molecular layers between graphene sheets and the insertion provides the variation of many properties. Alkali-metal GICs (AGICs) show two-dimensional high conductivity that can be easily controlled by changing number of intercalated metal layers, through charge transfer from *s* band of intercalated alkali-metal atoms to C 2*p* π band residing on the graphene layers, and some of them exhibit superconductivity. The interests in low-dimensional systems have lead to numbers of studies for the electronic structure and electric properties of GICs.[1–5] Since the discovery of AGIC superconductor C_8K, several superconducting GICs have been reported. However, their superconducting transition temperatures (T_c's) are generally low (<2 K).[6,7] Therefore, the discovery of a new GIC superconductor CaC_6 exhibiting T_c of as high as 11.5 K,[8] which is twice of that of C_2Na (=5 K),[9] the highest T_c before the discovery of CaC_6, has provoked much attention. This, together with a suggestion of exotic mechanism of superconductivity,[10] leads to numbers of experimental[11–13] and theoretical[14–18] studies to explore the origin of such a high T_c of CaC_6.

In nonsuperconducting AGICs, it is considered that the intercalated alkali metals give all the *s* electrons to the graphene layers, and the density of states (DOS) at the Fermi level (E_F) has only a C 2*p* character.[2,3,19] In contrast, in superconducting AGICs, the intercalated alkali metals are incompletely ionized and, therefore, DOS at E_F is composed of both *s* band derived from alkali metal and π band derived from graphite.[2–4] For CaC_6, the theoretical studies suggest that CaC_6 has an interlayer band near E_F, which has a Ca 3*d* character.[14–18] Since previous superconducting AGICs do not possess *d* states at E_F, the Ca 3*d* states at E_F are unique and therefore important to realize such a high T_c, as has been discussed.[18] Very recently, angular-resolved photoemission study showed the interlayer band induced by Ca intercalation and its relation to superconductivity.[13] However, orbital character of states at E_F of CaC_6 remains experimentally not to be elucidated. Therefore, it is important to perform further photoemission spectroscopy in order to demonstrate Ca 3*d* states at E_F in CaC_6.

In this paper, we report soft x-ray photoemission spectroscopy (SXPES) of a Ca-intercalated graphite superconductor CaC_6 (=11.2 K) in order to experimentally elucidate Ca 3*d* states at E_F. A valence-band spectrum has, besides several structures that can be related to those of graphite, a sharp peak at E_F. A comparison with band calculations indicates that the sharp peak at E_F consists of C 2*p* states strongly hybridized with Ca 3*d* states. A Ca 2*p* core-level spectrum of CaC_6 shows a very asymmetric spectral shape, possibly suggesting existence of Ca 3*d* derived states at E_F. Moreover, resonant photoemission spectroscopy (RPES) shows that the intensity of the states at E_F is resonantly enhanced at the Ca 2*p*-3*d* threshold, providing direct spectroscopic evidence for the existence of Ca 3*d* electrons at E_F, which play a crucial role for the superconductivity. We also discuss differences and similarities in electronic structure at E_F between CaC_6 and other GICs, which may shed light on the origin of higher T_c of CaC_6.

II. EXPERIMENTAL

CaC_6 samples were prepared by reacting highly oriented pyrolytic graphite (HOPG) with a molten Li-Ca alloy at 350 °C for several hours.[20] T_c of 11.2 K was confirmed as an

onset of temperature-dependent magnetization measurements. Because of easy deterioration of CaC_6 by exposure to the air, the sample was glued to a sample holder under argon atmosphere. The sample was transferred to measurement chamber under the same condition. For comparison, we also measured HOPG.

The SXPES spectra of valence band and core level were measured using a photon energy of 1100 eV at BL25SU of SPring-8 with a Scienta SES200 electron analyzer. The energy resolution was set to be ~100 meV to obtain a reasonable count rate. Resonant photoemission spectroscopy was also performed at BL25SU of SPring-8 and the energy resolution was set to be 70 meV. The sample was cooled using a He-cycled cryostat down to 20 K. Clean surfaces for PES measurements were obtained by cleaving the sample under 5×10^{-8} Pa. E_F of the sample was referenced to that of a Au film which was measured frequently during the experiments.

Band-structure calculations for CaC_6 are performed by the first-principles full-potential linearized augmented plane-wave method within the local-density approximation. Methodological details follow those used in the previous calculation.[21] The result is consistent with previous studies.[14–18]

III. RESULTS AND DISCUSSION

Figure 1 shows valence-band SXPES spectra of CaC_6 and HOPG measured with 1100 eV photon energy, together with calculated DOS of CaC_6. In our SXPES spectrum of CaC_6, we find six structures denoted with A-F. Note that an increase in intensity on the higher binding-energy side of structure F is due to the shallow core level of Ca 3*p* at 26 eV. We compared the SXPES spectrum of CaC_6 with the calculated total and partial DOS, which are energy expanded by 10% to fit the total band (light green) width below E_F to that of the SXPES spectrum. This empirically determined band expansion implies the introduction of self energy whose real part has linear energy dependence from E_F. As indicated with the vertical solid lines, the observed six structures correspond to structures in the calculated DOS, where the structures E and F are constructed by partial DOS (PDOS) mainly derived from C 2*s*, the structures B and C are dominated by those derived from C 2*p*, and the structure D consists of those derived from both C 2*s* and C 2*p* (the structure A will be discussed later). In comparison with the spectrum of HOPG in Fig. 1, it is found that the structures B-F can be related to those of HOPG (as shown with broken lines), although energy separation between structures B and C of CaC_6 is smaller than that of corresponding structures at 3 and 8 eV in HOPG.[22] This means that the electronic structure of CaC_6 is not obtained by a simple rigid-band shift of the electronic structure of graphite. (One could explain that the energy separation between the top of π band and the bottom of the σ band in graphite is smaller due to intercalation in CaC_6, see Fig. 1 in Ref. 16.)

As a result of Ca intercalation, a new pronounced structure labeled by A appears near E_F and no corresponding structure is seen in HOPG spectrum. This is clearly different from very small intensity at E_F observed for a nonsuperconducting AGIC, LiC_6, for which the experimental results show that the Li 2*s* band is unoccupied.[2,3,19] In contrast, for superconducting AGICs (KC_8, RbC_8, CsC_8), similar enhancement of DOS near E_F are observed and it is concluded that the conduction band is mainly due to *s* states of the intercalant.[2–4] For CaC_6, the calculated DOS in Fig. 1 shows that the electronic structure near E_F, which is important for superconductivity, consists of PDOS derived from C 2*p* and Ca 3*d* with negligible contributions of Ca 4*s* and C 2*s* (the calculated PDOS ratio at E_F of C 2*p*:Ca 3*d*:Ca 4*s*:C 2*s* = 125:45:5:2).

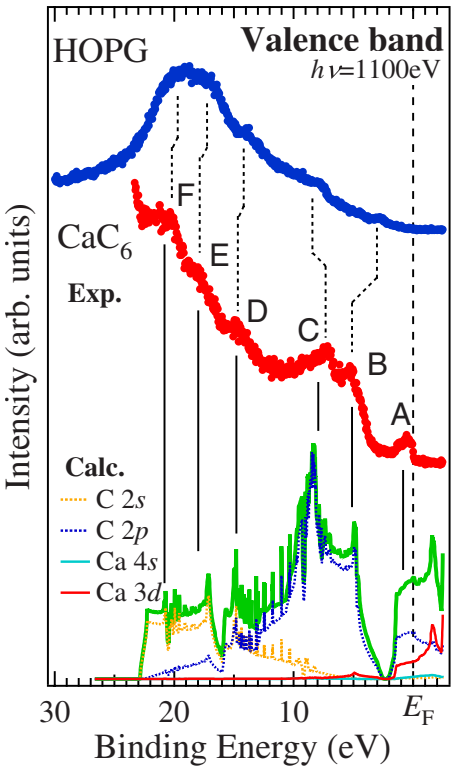

FIG. 1. (Color online) Valence-band SXPES spectra from CaC_6 (red/gray circles) and HOPG (blue/dark gray circles) using 1100 eV, together with calculated DOS. Green line is total DOS. Broken lines are partial DOS from C 2*s* (orange/light gray) and C 2*p* (blue/dark gray). Thin lines are partial DOS from Ca 4*s* (sky blue/light gray) and Ca 3*d* (red/gray).

To more directly evince the existence of substantial Ca 3*d* states at E_F, we have performed RPES using a Ca $2p_{3/2}$ absorption edge. Figure 2(a) shows the Ca $2p_{3/2}$ (L_3) absorption spectrum of CaC_6. The absorption spectrum displays the local unoccupied Ca 4*s* and 3*d* states due to the dipole selection rules of the x-ray absorption process. The Ca $2p_{3/2}$ (L_3) absorption spectrum is composed of a peak at photon energy 348.6 eV with an additional weak structure at the onset. The multiple structures are similar to the 2*p*-3*d* absorption spectrum of Ca metal,[23] indicating that the Ca $2p_{3/2}$ absorption spectrum of CaC_6 dominantly comes from the Ca 2*p*-3*d* absorption. Thus, by RPES using the photon energy at the Ca $2p_{3/2}$ absorption edge, states with a Ca 3*d* character should be enhanced. In Fig. 2(b), we show valence-band spectra of a near E_F region measured with photon energies around the Ca $2p_{3/2}$ absorption edge. Here the labels on the

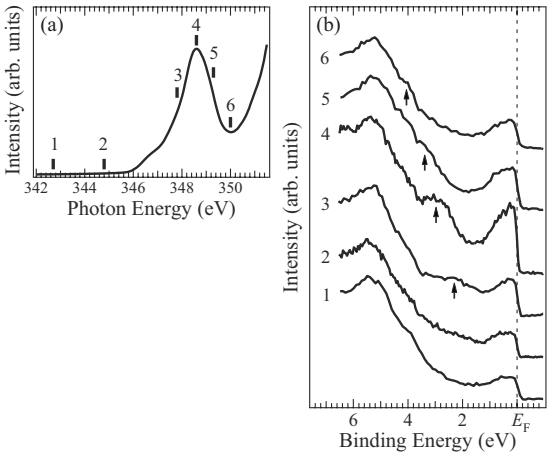

FIG. 2. RPES using the Ca $2p_{3/2}$ (L_3) absorption edge. (a) The Ca $2p_{3/2}$ absorption edge of CaC_6. The labels on the spectra (1–6) correspond to photon energies for photoemission. (b) Valence band spectra of CaC_6 measured using photon energies near Ca $2p_{3/2}$ absorption edge. The arrows indicate the Auger transition.

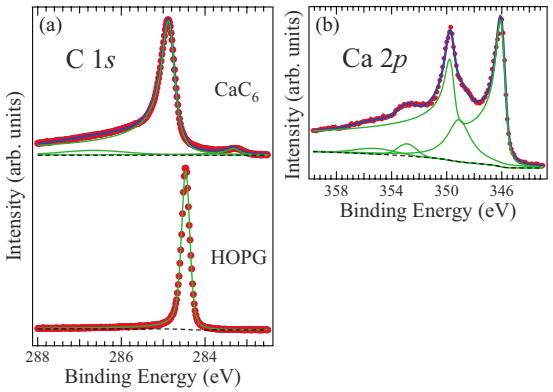

FIG. 3. (Color online) Core-level SXPES spectra of (a) C 1s of CaC_6 and HOPG as well as (b) Ca 2p of CaC_6. Circles are the experimental data, blue/dark gray thick lines are the fitting results, green/light green thin lines are the components used for the fittings, and black broken lines are background.

spectra (1–6) correspond to photon energies indicated in Fig. 2(a). Note that a new peak of curves 3–6, which is denoted with an arrow on Fig. 2(b), is characterized by an Auger signal, evidenced from a photon energy dependent change in its energy position. It is clearly seen that the RPES intensity is appreciably enhanced in the close vicinity of E_F for the on-resonant spectrum (curve 4) and exhibits the resonant behavior. As the photon energy is increased from 1 to 4, the near E_F peak intensity increases, reaching its maximum at the photon energy of the absorption maximum (curve 4). Then, it decreases at higher photon energies (curves 5 and 6). This result means that Ca 3d states *do* exist at E_F, as suggested from the band calculation and a spectral analysis of Ca core-level discussed later. Existence of Ca 3d states at E_F is consistent with specific-heat measurements showing that the electronic contribution of specific heat γ of CaC_6 (Ref. 10) is ten times greater than that of the superconducting AGICs.[3,24]

In Fig. 3, we show core-level spectra of C 1s and Ca 2p of CaC_6 as well as that of C 1s of HOPG. The C 1s spectrum of CaC_6 shows a main peak at 284.9 eV with a tail to a higher binding-energy side (around 287 eV) and a small peak at 283.2 eV. The tail and the small peak in CaC_6 are surface components, as their intensities relative to that of the main peak were increased in more surface sensitive SXPES using 500 eV photon energy (not shown). In the binding-energy region of the tail structure, there are components due to adsorbed C-O contaminations.[25] A lower binding-energy structure compared to a C 1s main peak was reported in C 1s spectrum of Al evaporated onto a graphite surface.[26] Thus we speculate that the small peak may be due to remaining Li- or Ca-graphite compounds on the surface. The main peak position of CaC_6 (284.9 eV) is higher than that of HOPG (284.5 eV) where the energy shift is nearly the same as that of structures D-F in their valence band and may be explained by the increase in chemical potential. The C 1s main peak spectral shape of CaC_6 is broader and more asymmetric than that of HOPG. For the Ca 2p peak, the spectrum show an asymmetric spin-orbit doublet peak at 349.7 eV (Ca $2p_{1/2}$) and 346.1 eV (Ca $2p_{3/2}$) with several weaker structures around 348.5, 353, and 355.5 eV. The weaker structures can be assigned as plasmon peaks since their relative energy separation of ~3 eV from the main peaks are close to the calculated value. We also compared Ca 2p of CaC_6 with those of calcium metal and other calcium compounds[27] and found that binding energy of Ca $2p_{3/2}$ (E_B=346.1 eV) of CaC_6 is closer to that of calcium metal (E_B=345.9 eV) than that of ionic compounds such as CaO (E_B=347.1 eV).

In order to prove the charge transfer and the existence of substantial Ca 3d PDOS at E_F, we have tried curve fittings using an asymmetric function (Doniach-Sunjic function) for main peaks and Voigt functions for other structures. It is known that such an asymmetric core-level spectral shape can be explained by Mahan-Nozières-De Dominicis effect,[28,29] which comes from a core-hole screening by the conduction electrons and is thus more evident for metallic samples. Singularity index α shows a degree of asymmetry in a core-level spectrum due to this effect and the value depends on the numbers of conduction electrons as well as the type of orbital concerned. Here we obtained singularity indices of 0.39 for Ca 2p, 0.25 for C 1s of CaC_6, and 0.05 for C 1s of HOPG.[30] The singularity indices of Ca 2p and C 1s in CaC_6 imply that there are PDOS at E_F from each atom. For the C 1s spectra, the singularity index increases from 0.05 (HOPG) to 0.25 (CaC_6) when Ca is intercalated into graphite. This consistently explains the experimental observations which are the nearly symmetric line shape of semi-metallic HOPG having a zero DOS at E_F and the asymmetric line shape of metallic CaC_6 having a DOS peak at E_F. This means that, upon Ca intercalation, the number of conduction electrons screening the core holes increases due to buildup of C-derived DOS at E_F, which is induced by the charge transfer from Ca to graphene layers. From the comparison of singularity indices of Ca and C, we found that the singularity index of Ca 2p is larger than that of C 1s in spite of smaller PDOS at E_F of Ca 3d than C 2p. In Ca metal, numerical self-consistent field calculations predict that the conduction electrons derived from Ca 3d electrons can make singularity

index large and indeed give a singularity index of Ca in Ca metal (α=0.35) (Ref. 31) similar to that in CaC_6. This effect may overcome the smaller PDOS of Ca 3*d* at E_F than that of C 2*p*. In contrast, singularity indices of sodium, magnesium, and aluminum (α_{Na}=0.15–0.2, α_{Mg}=0.13–0.15, and α_{Al} =0.10–0.16) (Ref. 31) without *d*-derived PDOS at E_F are almost half as large as that of Ca in CaC_6. If Ca in CaC_6 has only conduction 4*s* electrons, it is expected that the singularity index of Ca 2*p* is almost the same as above simple metals. These results support that there might be Ca 3*d*-derived PDOS at E_F in CaC_6.

Here a comparison with other GICs is essential to clarify the similarity and difference in their electronic structures. As mentioned above, electronic structure of nonsuperconducting GICs is known to be described with simple rigid-band shift of graphite. Intercalated atoms are fully ionized to give electrons to graphite layers. Thus, DOS at E_F are derived from C 2*p* orbitals. These are different from those of CaC_6. In the superconducting AGICs (C_8K, C_8Rb, and C_8Cs), near E_F electronic structure is derived from C 2*p* and alkali-metal *s* electrons, indicating incomplete ionization of alkali metals.[2–4] Incomplete ionization of intercalated atoms and both the C atom and intercalated atom derived states at E_F are the same as CaC_6. However, we come to understand a crucial difference between CaC_6 and the traditional superconducting AGICs; CaC_6 has PDOS at E_F due to Ca 3*d* electrons while the traditional AGICs have no conduction *d* electrons. Recently, it was reported that YbC_6 has a T_c of 6.5 K (Ref. 8) and ARPES observed that Yb-GIC has 5*d*-derived PDOS at E_F but without confirming its composition and superconductivity.[5] Thus, in terms of electronic structure, CaC_6 and YbC_6 can be classified as a type of GICs, where *d* electrons play an important role for the conducting properties including superconductivity at relatively high T_c. This is consistent with the recent theoretical studies by Zhang *et al.*[18] suggesting that increase in *d* electrons leads to enhanced T_c.

IV. CONCLUSIONS

We have performed high-resolution soft x-ray photoemission spectroscopy on a graphite-intercalation superconductor CaC_6 in order to study the electronic structure. From the valence-band spectra, we found that valence band of CaC_6 is closely related to the calculated DOS of CaC_6 that predicts Ca 3*d*-derived DOS at E_F but different from a rigid-band shift of the electronic structure of graphite. We observed the asymmetric spectral shape of core levels (Ca 2*p* and C 1*s*), maybe suggesting that Ca 3*d*-derived states are located at E_F. A more direct spectroscopic evidence of Ca 3*d* character of states at E_F was provided from resonant photoemission spectroscopy using the Ca $2p_{3/2}$ absorption edge. The existence of Ca 3*d*-derived states at E_F is unique to CaC_6, suggesting close correlation with its relatively high T_c. New GIC superconductors having a T_c higher than that of CaC_6 may be realized among transition-metal GICs.

ACKNOWLEDGMENTS

We thank Y. Kubozono, Y. Ohta, and N. Kawasaki for sample preparation. We also thank K. Okada for valuable discussions. This work was supported partly by a Grant-in-Aid for Scientific Research of the Ministry of Education, Culture, Sports, Science and Technology, Japan. The PES measurements at SPring-8 were performed under a Proposal No. 2008A1740.

[1] M. S. Dresselhaus and G. Dresselhaus, Adv. Phys. **51**, 1 (2002).
[2] T. Enoki and K. Suzuki, Netsu Sokutei **15**, 185 (1988).
[3] U. Mizutani, T. Kondow, and T. B. Massalski, Phys. Rev. B **17**, 3165 (1978).
[4] P. Oelhafen, P. Pfluger, E. Hauser, and H.-J. Guntherodt, Solid State Commun. **33**, 241 (1980).
[5] S. L. Molodtsov, C. Laubschat, M. Richter, Th. Gantz, and A. M. Shikin, Phys. Rev. B **53**, 16621 (1996).
[6] N. B. Hannay, T. H. Geballe, B. T. Matthias, K. Andres, P. Schmidt, and D. MacNair, Phys. Rev. Lett. **14**, 225 (1965).
[7] I. T. Belash, A. D. Bronnikov, O. V. Zharikov, and A. V. Pal'nichenko, Solid State Commun. **69**, 921 (1989).
[8] T. E. Weller, M. Ellerby, S. S. Saxena, R. P. Smith, and N. T. Skipper, Nat. Phys. **1**, 39 (2005).
[9] I. T. Belash, A. D. Bronnikov, O. V. Zharikov, and A. V. Palnichenko, Solid State Commun. **64**, 1445 (1987).
[10] G. Csányi, P. B. Littlewood, A. H. Nevidomskyy, C. J. Pickard, and B. D. Simons, Nat. Phys. **1**, 42 (2005).
[11] J. S. Kim, R. K. Kremer, L. Boeri, and F. S. Razavi, Phys. Rev. Lett. **96**, 217002 (2006).
[12] N. Bergeal, V. Dubost, Y. Noat, W. Sacks, D. Roditchev, N. Emery, C. Hérold, J-F. Marêché, P. Lagrange, and G. Loupias, Phys. Rev. Lett. **97**, 077003 (2006).
[13] K. Sugawara, T. Sato, and T. Takahashi, Nat. Phys. **5**, 40 (2008).
[14] I. I. Mazin, L. Boeri, O. V. Dolgov, A. A. Golubov, G. B. Bachelet, M. Giantomassi, and O. K. Andersen, Physica C **460-462**, 116 (2007).
[15] S. Deng, A. Simon, and J. Köhler, Angew. Chem., Int. Ed. **47**, 6703 (2008).
[16] L. Boeri, G. B. Bachelet, M. Giantomassi, and O. K. Andersen, Phys. Rev. B **76**, 064510 (2007).
[17] M. Calandra and F. Mauri, Phys. Rev. Lett. **95**, 237002 (2005); Phys. Rev. B **76**, 161406(R) (2007).
[18] L. Zhang, Y. Xie, T. Cui, Y. Li, Z. He, Y. Ma, and G. Zou, Phys. Rev. B **74**, 184519 (2006).
[19] G. K. Wertheim, P. M. Th. M. V. Attekum, and S. Basu, Solid State Commun. **33**, 1127 (1980).
[20] M. Toyoda, A. Takenaka, Y. Takano, A. Yoshida, Y. Kaburagi, and N. Akuzawa, Trans. Am. Nucl. Soc. **233**, 148 (2008).
[21] T. Oguchi, J. Phys. Soc. Jpn. **71**, 1495 (2002).
[22] This is consistent with the fact that the calculated band width derived from C 2*p* in CaC_6 is smaller than that in graphite. J. Schäfer, J. Ristein, R. Graupner, L. Ley, U. Stephan, Th. Frauenheim, V. S. Veerasamy, G. A. J. Amaratunga, M. Weiler, and H. Ehrhardt, Phys. Rev. B **53**, 7762 (1996).
[23] F. J. Himpsel, U. O. Karlsson, A. B. McLean, L. J. Terminello, F.

M. F. de Groot, M. Abbate, J. C. Fuggle, J. A. Yarmoff, B. T. Thole, and G. A. Sawatzky, Phys. Rev. B **43**, 6899 (1991).

[24] M. Suganuma, T. Kondow, and U. Mizutani, Phys. Rev. B **23**, 706 (1981).

[25] J. F. Moulder, W. F. Stickle, P. E. Sobol, and K. D. Bomben, *Handbook of X-ray Photoelectron Spectroscopy* (Physical Electronic, Inc., Minnesota, 1995).

[26] C. Hinnen, D. Imbert, J. M. Siffre, and P. Marcus, Appl. Surf. Sci. **78**, 219 (1994).

[27] M. I. Sosulnikov and Y. A. Teterin, J. Electron Spectrosc. Relat. Phenom. **59**, 111 (1992).

[28] G. D. Mahan, Phys. Rev. **163**, 612 (1967).

[29] P. Nozières and C. T. De Dominicis, Phys. Rev. **178**, 1097 (1969).

[30] For this analysis, one should pay attentions to the existence of additional contributions that can change significantly lineshapes of core-level spectra in the energy range of simulation. In the case of the Ca 2*p* spectra, these changes stem from the plasmon losses. But, the plasmon contributions are taken into considerations in the lineshape analysis, as shown in Fig. 3(b). We find that, for the better fit, the linewidth of the components can not be varied very much, giving rise to a small error bar ($\pm 10\%$) of the alpha value. Additional lineshape changes both in the Ca 2*p* and C 1*s* signals may be caused by contaminations and/or nonstoichiometric C. Nonstoichiometric C contribution might gives Gaussian contribution to the lineshape. For the possibility of contaminations, we find that O core-level signals, other than C and Ca core levels, from the wide energy-range scan. We estimated that the ratios of spectral intensity of O 1*s* to those of Ca 2*p* and C 1*s* are less than 5%, which does not change the estimated alpha value significantly.

[31] T. T. Rantala, Phys. Rev. B **28**, 3182 (1983).